This article was downloaded by: [University of Haifa Library]
On: 20 August 2012, At: 10:37
Publisher: Taylor & Francis
Informa Ltd Registered in England and Wales Registered Number: 1072954
Registered office: Mortimer House, 37-41 Mortimer Street, London W1T 3JH, UK

Molecular Crystals and Liquid Crystals Science and Technology. Section A. Molecular Crystals and Liquid Crystals

Publication details, including instructions for authors and subscription information:
http://www.tandfonline.com/loi/gmcl19

Electric Field Induced Walls in the Bend Geometry of a Nematic Liquid Crystal

Shila Garg [a] , Erica Bramley [a c] & U. D. Kini [b]

[a] Department of Physics, The College of Wooster, Wooster, Ohio, 44691, USA

[b] Raman Research Institute, Bangalore, 560 080, India

[c] Physics Department, Colorado State University, Fort Collins, CO, 80523

Version of record first published: 24 Sep 2006

To cite this article: Shila Garg, Erica Bramley & U. D. Kini (1998): Electric Field Induced Walls in the Bend Geometry of a Nematic Liquid Crystal, Molecular Crystals and Liquid Crystals Science and Technology. Section A. Molecular Crystals and Liquid Crystals, 325:1, 209-240

To link to this article: http://dx.doi.org/10.1080/10587259808025396

PLEASE SCROLL DOWN FOR ARTICLE

Full terms and conditions of use: http://www.tandfonline.com/page/terms-and-conditions

This article may be used for research, teaching, and private study purposes. Any substantial or systematic reproduction, redistribution, reselling, loan, sub-licensing, systematic supply, or distribution in any form to anyone is expressly forbidden.

The publisher does not give any warranty express or implied or make any representation that the contents will be complete or accurate or up to date. The accuracy of any instructions, formulae, and drug doses should be independently verified with primary sources. The publisher shall not be liable for any loss, actions, claims, proceedings, demand, or costs or damages whatsoever or howsoever caused arising directly or indirectly in connection with or arising out of the use of this material.

Downloaded by [University of Haifa Library] at 10:37 20 August 2012

Mol. Cryst. Liq. Cryst., Vol. 325, pp. 209–240
Reprints available directly from the publisher
Photocopying permitted by license only

© 1998 OPA (Overseas Publishers Association) N.V.
Published by license under
the Gordon and Breach Science
Publishers imprint.
Printed in Malaysia.

Downloaded by [University of Haifa Library] at 10:37 20 August 2012

Electric Field Induced Walls in the Bend Geometry of a Nematic Liquid Crystal

SHILA GARG[a,*], ERICA BRAMLEY[a,†] and U. D. KINI[b]

[a] *Department of Physics, The College of Wooster, Wooster, Ohio 44691, USA;*
[b] *Raman Research Institute, Bangalore 560 080, India*

(Received 21 January 1998; In final form 9 July 1998)

A homeotropically aligned nematic is subjected to the action of an ac electric field applied in the sample plane. With progressively increasing electric voltage, walls move away from the electrodes, approach each other and merge. A subsequent decrease of voltage to zero causes the reverse process to occur except for hysteresis. The hysteresis width is employed to estimate the adhesion surface energy density of the walls; the surface energy density is of the same order as the anisotropy in surface tension of nematics. The wall thickness diminishes with increasing voltage. This shows that the observed walls are similar to those produced by magnetic fields. The walls exhibit curvature in the sample plane, the undulation in a wall being regular at sufficiently elevated frequencies (f). The walls are decorated along their length by a zigzag defect pattern which is being reported in the bend Freedericksz geometry for the first time. Some of the observations are explained qualitatively.

Keywords: Nematic; electric field; bend geometry; zigzag disclinations; alignment inversion walls; Freedericksz transition

1. INTRODUCTION

Over the last several decades, the optical observation of defects in a liquid crystal sample has been an important technique for identifying the nature of the mesophase [1]. The study of director deformation at and around defects has occupied the attention of many theoretical investigations (for a review, see [2]). Of the several kinds of textures that are studied, the alignment

* Corresponding author. e-mail: sgarg@acs.wooster.edu
† Present address: Physics Department, Colorado State University, Fort Collins, CO 80523.

Downloaded by [University of Haifa Library] at 10:37 20 August 2012

inversion walls (or walls) in nematics are some of the commonest. These generally form when the nematic sample is subjected to the action of external fields, especially above a Freedericksz transition. The investigation of Williams [3] was followed by Helfrich's theoretical treatment [4] for an infinite sample subjected to the action of a magnetic field. Subsequent studies by Brochard [5] and Leger [6] have given further insight into the nature of walls that separate adjacent regions having director deformations of opposite parity above a magnetic Freedericksz transition. The effect of an electric field is generally more complex as the field gets modified inside the sample due to the director deformations. This may lead to new effects such as the splitting of a single wall into different parts as observed by Stieb *et al.* [7] in the splay Freedericksz geometry under the action of an electric field (the initial director alignment is parallel to the sample plates; the voltage is applied between semi-transparent conducting electrodes coated on the inside surfaces of the sample plates). Zigzag disinclination lines have also been reported [8–10] in nematics confined to different configurations. These defect lines are localized in regions of the sample that are removed from the sample boundaries.

The bend Freedericksz geometry (initial homeotropic director alignment subjected to an electric field in the sample plane) has also been studied. Frisken and Palffy-Muhoray [11] have demonstrated a first order Freedericksz transition accompanied by hysteresis and also detected a periodic deformation in the presence of a stabilizing magnetic field. Several other observations have been reported in this configuration [12–14]. The deformation sets in without a threshold near the electrodes and spreads inward with increasing voltage. Depending upon the stabilizing magnetic field and the electric frequency, the initial deformation undergoes instabilities leading to either static or convective pattern formation. Not surprisingly, wall formation in this geometry shows novel features not ordinarily seen in the splay Freedericksz geometry. We first summarize the recent observations of Schell and Porter [12], whose samples are similar to those employed by us (Fig. la).

Schell and Porter [12] study the material 5*CB* using electrodes of different shapes as well as sample thicknesses in the range 2.5 to 42 μm. With increasing voltage, they observe birefringent regions near the electrodes with a relatively undistorted (homeotropic) region in the rest of the sample. When the voltage is increased further, each birefringent region develops a wavy front. The wavy fronts approach each other as the voltage is enhanced. At a sufficiently elevated voltage, these fronts coalesce midway between the electrodes leaving a straight wall. A subsequent diminution in voltage drives

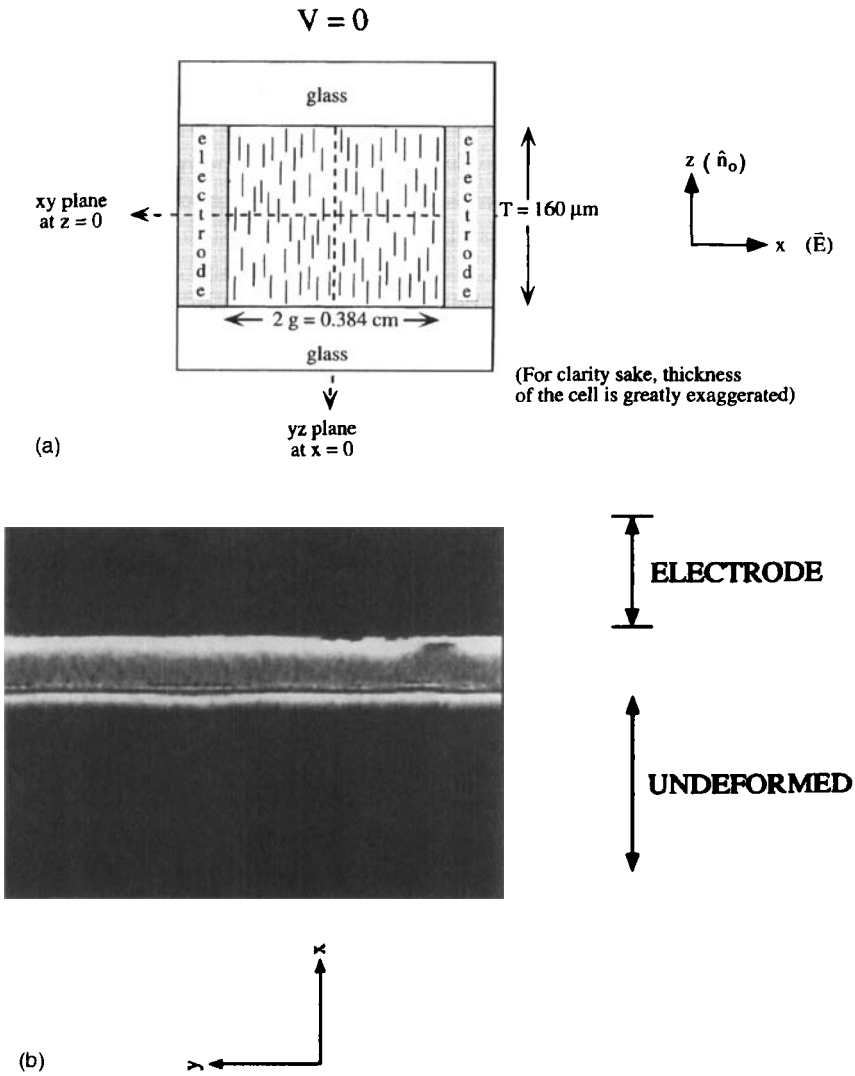

FIGURE 1 (a) Sample (not drawn to scale). The initial director alignment is along z, normal to the glass plates. The electrodes are plane metal plates that lie in the yz plane. (b) Straight edge of the boundary between the deformed and undeformed regions near one electrode. $f = 1500$, $V = 26.06$. Magnification (M) = 110. (See Color Plate XI).

the system through the reverse cycle. The wavy pattern is more stable at higher frequencies. The authors offer a tentative explanation for their observations using the criteria for electrohydrodynamical stability developed for the initial planar orientation [15].

Downloaded by [University of Haifa Library] at 10:37 20 August 2012

Downloaded by [University of Haifa Library] at 10:37 20 August 2012

The motivation for our work is provided by some questions that arise after a study of [12]. The electric field induced transitions in the bend Freedericksz geometry are generally accompanied by hysteresis [11, 13, 14]. Does hysteresis manifest in the effect studied in [12]? In other words, after the fronts have coalesced, do they separate when the voltage is diminished even slightly? This question becomes significant if we take seriously the fluid nature of the coalescing fronts and the force of adhesion that may exist between them. What is the effect of applying a stabilizing magnetic field? It is known that a stabilizing magnetic field enhances the electric Freedericksz threshold. This also means that a distortion initially produced by a destabilizing electric field may be quenched by the subsequent application of a stabilizing magnetic field. Let us assume that the coalescence of the fronts at some voltage is regarded as a threshold effect. If we apply a strong stabilizing magnetic field, can we take the system back to the undeformed state (*i.e.*, can we drive the fronts back to the electrodes)? Do the walls that appear undergo splitting (as they do in [7])? It should also be interesting to find out whether the results of [12] can be completely recovered in thicker samples.

Section 2 describes the experimental set up utilized by us as well as the main results. All observations reported in Section 2 were found to be repeatable. Section 3 contains qualitative discussions that are based on some of the observations of Section 2. Section 4 contains the main conclusions of this work as well as suggestions for future experiments that may be useful in providing a more complete understanding of our results.

2. EXPERIMENTAL SETUP AND RESULTS

The cell of thickness $T = 160\,\mu m$ (Fig. 1a) is constructed by sandwiching two glass plates (in the xy plane) with brass electrodes which also serve as spacers. The flat surfaces of the electrodes (in the yz plane at $x = \pm g$) are parallel to one another and separated by a gap of $2g = 0.384\,cm$. The lateral width of the sample (parallel to the electrodes) is $p = 2.62\,cm$. The initial homeotropic alignment (along z) is achieved by treating the inside surfaces of the glass plates with silane solution. The solution is prepared by filtering a mixture of 1 ml of silane, 25 ml isopropyl alcohol and 75 ml distilled water through a 0.2 micropore filter. Optical observations are performed using a Nikon Optiphot polarizing microscope. The incident and transmitted beams pass through polarizers with axes along y (parallel to the electrodes) and x, respectively. The video data collected by the Javelin camera mounted on the

Downloaded by [University of Haifa Library] at 10:37 20 August 2012

microscope is sent to the video board of a Macintosh 8500 computer and digitized. The ac signal produced by a Hewlett Packard function generator is fed to a Kepco bipolar amplifier before being applied across the cell. The voltage (measured in volts *rms*) is ramped quasistatically at a rate of $3.3\,10^{-3}$ V/s with equipment similar to the one described in [13]. The sample is maintained at 28.0 ± 0.1°C using the HS1 microscope hot stage supplied by Instec. As the electrode gap and the sample thickness are two different length scales, it is appropriate to mention the average electric field along x, rather than the electric potential difference. As the electrode gap is fixed for a given sample, we describe our observations using V.

When V is raised up from zero, the sample remains dark. When V exceeds a threshold V_a, a cloudy region forms near one electrode and starts spreading away from the electrodes when V is increased further. This corresponds to the birefringent region observed previously [12] and is clear proof of the inhomogeneity in the electric field (if we move parallel to the x axis from one electrode to the other, the electric field does not remain constant). When a deformation sets in near the electrode, the rest of the sample appears to be relatively undeformed. A similar, birefringent region appears near the other electrode at V slightly higher than V_a; this region also advances towards the plane at $x = 0$. The appearance of the two boundaries at slightly different voltages indicates the existence of some asymmetry in the sample. At V slightly above V_a, the boundaries between the deformed and undeformed regions appear as a pair of straight lines parallel to y; the line near one electrode is shown in Figure 1b. At a slightly higher voltage, V_b, the boundaries start exhibiting curvature and display sinusoidal modulation (Fig. 2) whose amplitude increases with V (Fig. 3). The boundary is visible as a curve lying in the xy plane. However, it can be seen clearly when the microscope is focused on different xy planes inside the sample. Hence, the boundary or front is a structure that spans the sample thickness from one glass plate to the other. The thick dark line seen under low magnification (Figs. 2 and 3) which also undergoes the transition to curvature with increasing voltage seems to be a wall similar to the ones studied in [5, 6] and [12]. A qualitative discussion of the nature of the director orientation in and around the wall is presented later in this section.

The wavy structure can be observed even with sufficiently low magnification and 10 to 15 wavelengths can be clearly seen when $f > 400$ Hz (f is measured in Hz throughout). This structure becomes uniform especially at higher frequencies, $f > 600$. When $f < 400$, the interface is wavy but somewhat nonuniform (Fig. 2a). The region enclosed by the wave has a fluctuating director orientation, the fluctuations becoming especially

Downloaded by [University of Haifa Library] at 10:37 20 August 2012

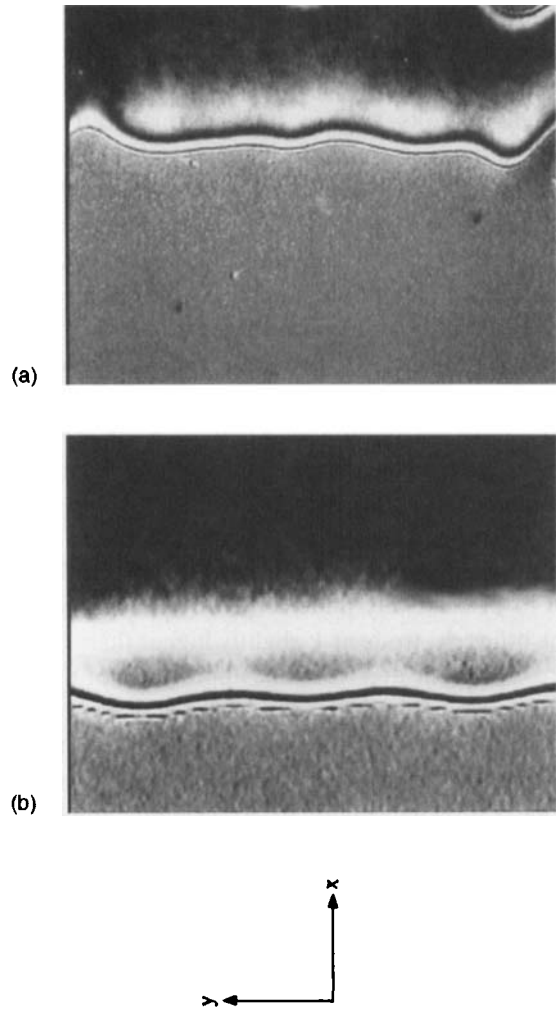

FIGURE 2 Appearance of curvature in the boundary between the deformed and undeformed regions when the voltage exceeds V_b. (a) $f = 400$, $V = 54.89$, $M = 57$. The waviness is nonuniform. (b) $f = 1500$, $V = 54.46$, $M = 110$. (See Color Plate XII).

apparent for $f < 20$. As the wave amplitude increases with V, the initially undeformed nematic in the region enclosed by the peaks undergoes distortion; this is evident from an increase in the birefringence. This growing deformation is clearly seen in Figure 3. These distortions grow with increasing V and merge as the wavefronts meet at different parts of the cell at slightly different voltages. The reason for this is that the two wavy fronts

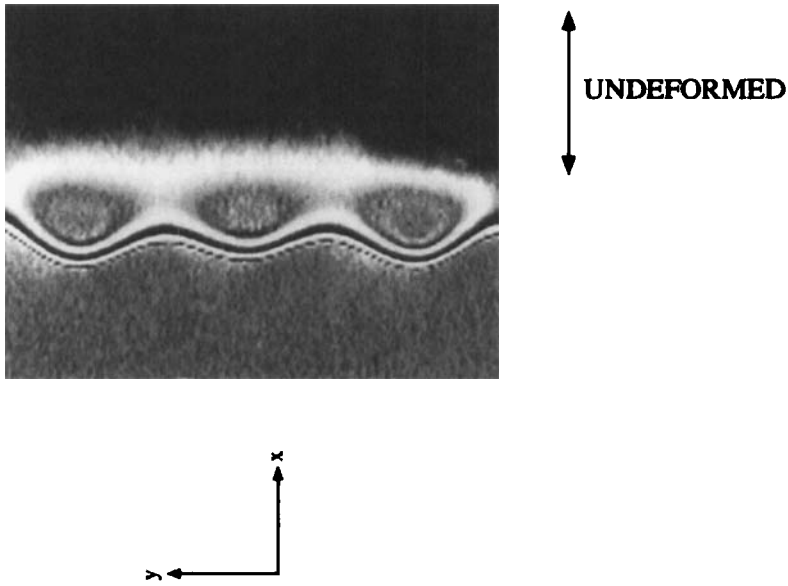

FIGURE 3 The amplitude of the sinusoidal modulation grows with voltage. $f = 1500$, $V = 55.49$, $M = 110$. (See Color Plate XIII).

that advance towards each other are not exactly out of phase along y. This is clearly seen in Figures 4a–d.

When the voltage is increased further, secondary bands appear on either side of the common front. Then at a still higher voltage, the common front near $x = 0$ becomes straight and then starts to dissolve. The speed of dissolution of the common front depends critically on the frequency. At high $f(= 1500)$, the front starts to dissolve very slowly. As the voltage is somewhat high, it is difficult to make observations for a long time without risking permanent damage to the cell. When f is low (say, 20 Hz), the common front oscillates in the xy plane before disappearing; the speed of dissolution is quite high compared to the high frequency case. The fact that the wavy structure cannot be observed at low f is in qualitative agreement with the earlier observations of [12] in that the presence of a lower cut-off frequency is indicated. In the previous work, the sample thickness had been varied between 2.5 and 42 μm; electrodes of different kinds had also been employed. Here we have demonstrated that similar effects can be observed even in thicker samples using flat electrodes.

For a given run involving either increase or decrease of V, the wavelength of modulation (λ) does not depend strongly on V. However, λ is noticeably

Downloaded by [University of Haifa Library] at 10:37 20 August 2012

higher when V is diminished than when V is augmented. For example, at $f = 1500$, $\lambda = 0.32 \pm 0.02$ mm during ramp up while $\lambda = 0.43 \pm 0.03$ mm during ramp down. The wavelength does not seem to depend on frequency in the frequency range over which the wavy structure is discernible. The waves stretch along y from one edge of the sample to the other. However,

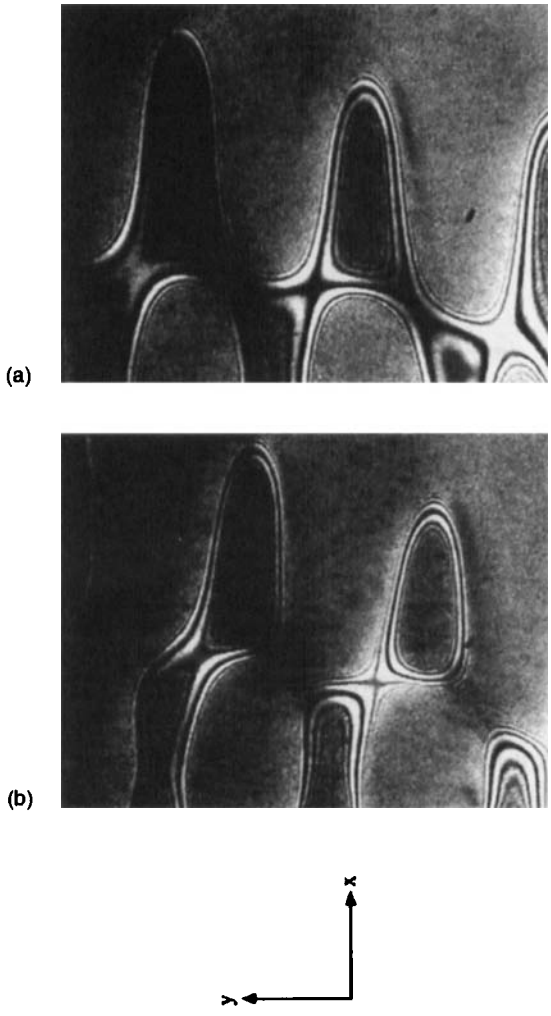

FIGURE 4 Magnified pictures of the coalescing fronts at $f = 1000$ and different voltages. Voltage ramp up. V = (a) 58.64 (b) 58.76, $M = 110$. Voltage ramp down. V = (c) 57.70, $M = 110$ (d) 57.22, $M = 57$. As the two fronts are not exactly out of phase, they do not merge at all places at a single voltage. The differences during voltage increase and decrease indicates hysteresis caused by the adhesion of the two surfaces. (See Color Plate XIV).

Downloaded by [University of Haifa Library] at 10:37 20 August 2012

Downloaded by [University of Haifa Library] at 10:37 20 August 2012

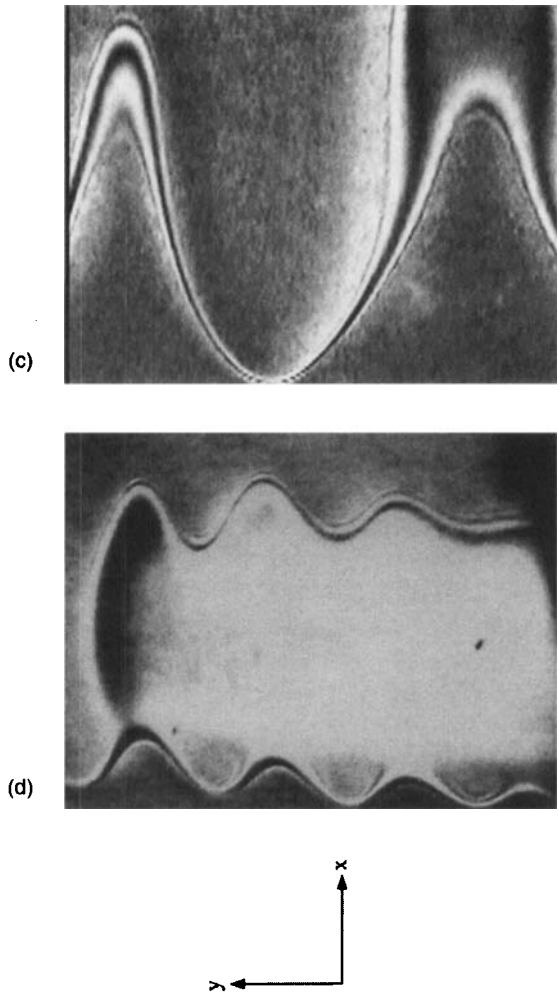

FIGURE 4 (Continued).

the waviness is perceptibly non-uniform close to the lateral edges which are sealed with epoxy.

From the time the wavy structure starts to form, the zigzag fine structure becomes noticeable all along the edge. Figure 5 show this microstructure at different levels of enlargement. Each pair of zigzag lines encloses a wall. It is seen that while the wall is a single dark curve close to the crests of the wavy front, it splits into two slightly lighter parts as we move away from the crests. This is especially evident at a higher magnification (Figs. 5b, d).

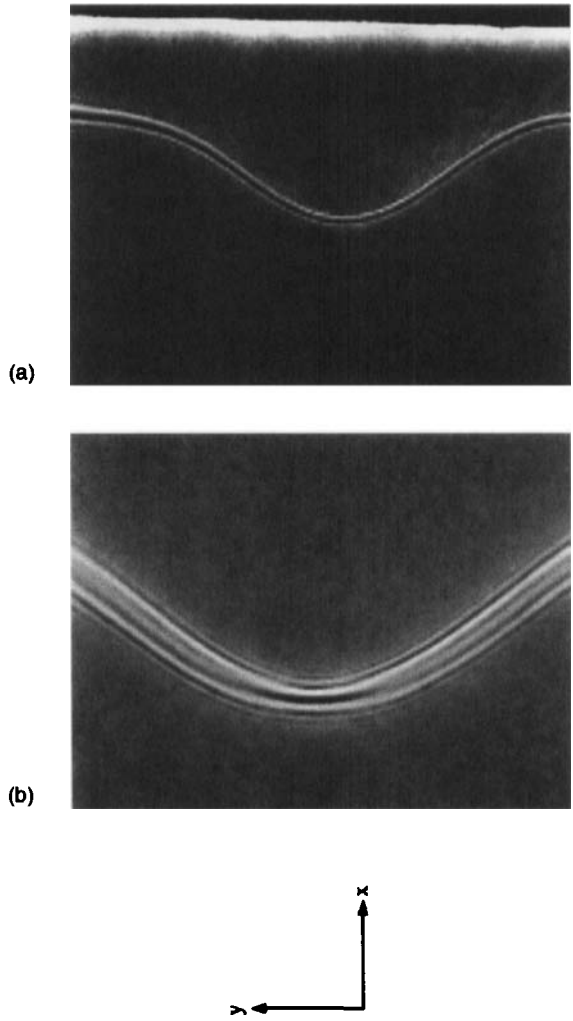

FIGURE 5 Magnified pictures of the zigzag fine structure. (a) $f = 5$, $V = 50.10$, $M = 110$ (b) $f = 5$, $V = 50.10$, $M = 220$ (c) $f = 400$, $V = 55.96$, $M = 110$ (d) $f = 1500$, $V = 58.28$, $M = 220$. (See Color Plate XV).

Measurements on Figures 2 and 5d show that the wall becomes perceptibly thinner with increasing voltage. This is qualitatively similar to the conclusions reached in [5] for walls that are observed above a magnetic Freedericksz transition. The qualitative difference from the case of the magnetic transition is this. As the electric field is inhomogeneous, two walls form more or less symmetrically between the electrodes and they both undergo wavelike deformation in the sample plane. In the magnetic case, the

Downloaded by [University of Haifa Library] at 10:37 20 August 2012

Downloaded by [University of Haifa Library] at 10:37 20 August 2012

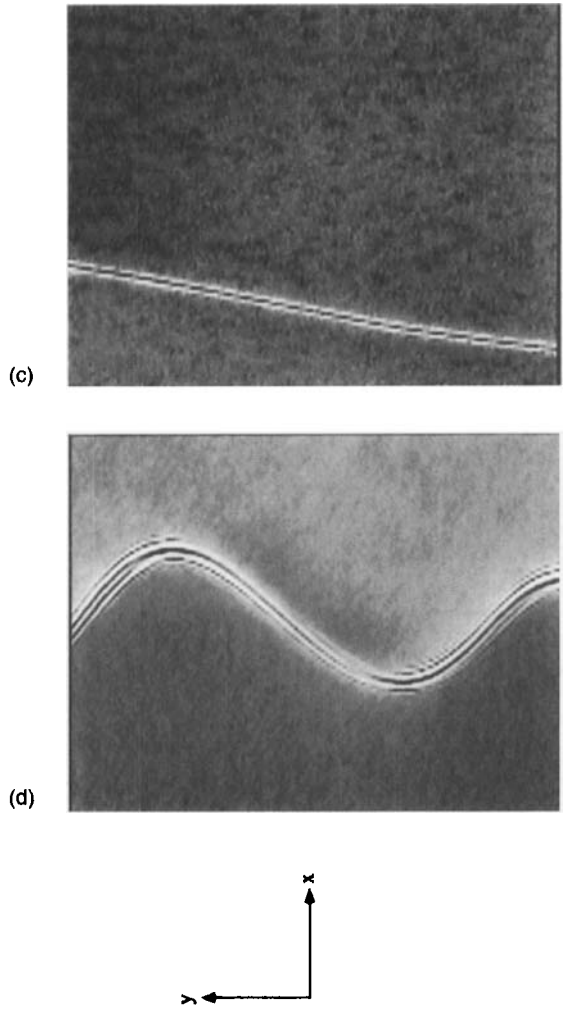

FIGURE 5 (Continued).

wall remains stationary for slow increments of the magnetic field. In the present case, the walls get pushed away from the electrodes with increasing voltage and merge near the plane at $x = 0$ (to avoid pedantic repetition, we use the term $x = 0$ to refer to the plane at $x = 0$).

The zigzags are static patterns. Even after the advancing wavy structures from the two electrodes coalesce into a single wavy structure near $x = 0$, the zigzags persist (Fig. 6). These patterns can be observed over a wide frequency range, say, $10 < f < 10^4$. They form the periphery of the interface that separates from either electrode. The separation between two adjacent

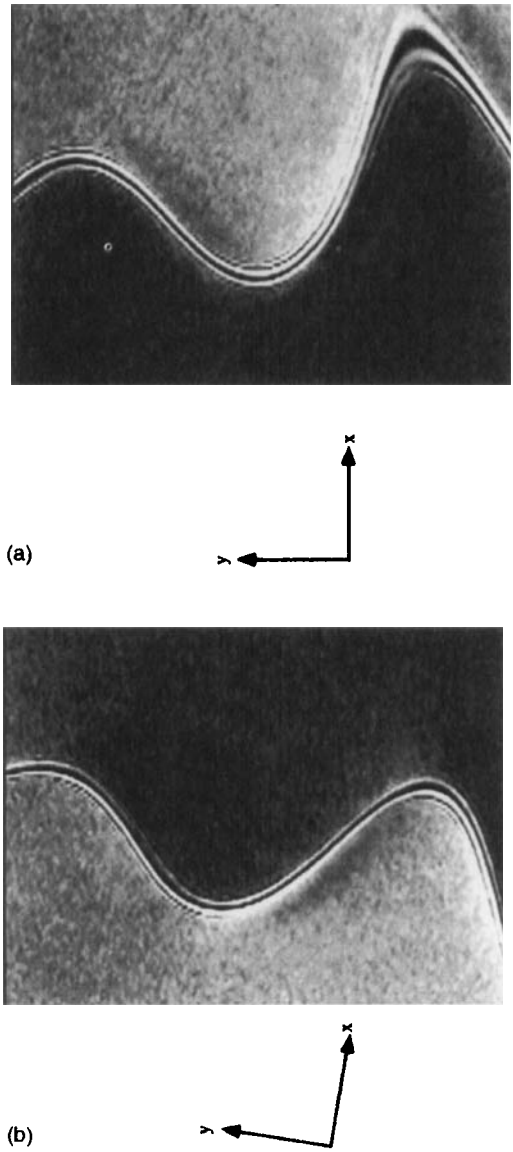

FIGURE 6 With increasing V, the wavy structures advance towards the plane at $x = 0$ and finally coalesce leaving a single wavy structure separating two domains with distinctly different birefringence. $f = 1500$, $V = 58.28$, $M = 57$. (a) and (b) are photographs taken when the platform is rotated through about 9°. (See Color Plate XVI).

dark spots on the zigzag can be regarded as the wavelength (λ'). Even at given f and V, λ' varies from 0.02 – 0.05 mm at different points on the wavy structure. However, λ' does not change appreciably with f or V.

Downloaded by [University of Haifa Library] at 10:37 20 August 2012

Under close inspection, each zigzag looks like a twisted rope of two strands with each strand coming into focus at a slightly different depth. With the polarizers crossed, the microscope platform is rotated so that one side of the zigzag appears bright and the other side dark (Fig. 6a). On further rotation of the platform through about 9°, the dark (or bright) domain becomes bright (or dark) as in Figure 6b. From this we conclude that the adjacent domains separated by the zigzag have a difference in director orientation of about 9° away from z at $f = 400$. When V is decremented, all the steps occur in the reverse order except for a hysteresis with regard to the appearance and disappearance of the wavy structure and the zigzag pattern (see Tab. I; also Figs. 4a–d). Figure 7 shows the interface on one side of the plane at $x = 0$ during the voltage ramp down; the zigzag pattern is seen clearly superposed on the wavy structure.

TABLE I Threshold voltage (in volts *rms*) for the *appearance* and *disappearance* of the wavy structure during *ramp up* and *ramp down*, respectively, at different frequencies (in Hz). The hysteresis width increases with frequency

Frequency	*Ramp up*	*Ramp down*	*Hysteresis*
500	52.83	51.25	1.58
600	53.99	51.90	2.09
1500	53.64	49.79	3.85

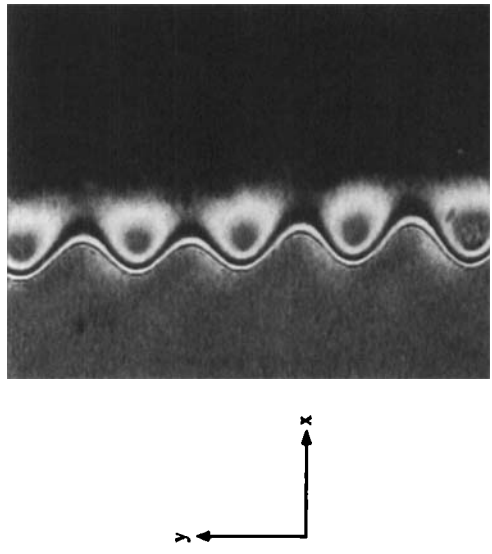

FIGURE 7 When V is diminished after coalescence, the wavy fronts separate. The figure shows one of the wavy structures. $f = 1500$, $V = 53.89$, $M = 57$. (See Color Plate XVII).

Downloaded by [University of Haifa Library] at 10:37 20 August 2012

Downloaded by [University of Haifa Library] at 10:37 20 August 2012

A parameter of interest that varies with the applied voltage is the position of either front. It should be instructive to plot this quantity as a function of V. As the electrostatic energy density as well as the dielectric torque generally vary as the square of the electric field, it is meaningful to plot the distance of each front from the respective electrode as a function of the squared voltage [12]. But this is not easy as the fronts are curved. One possibility is to fix a line parallel to y that is roughly midway between the extreme undulations of a given front and call this the *position of the front*. This definition may be useful at low voltages where the undulations on either front are sufficiently uniform. When the voltage increases and the fronts approach each other, the undulations become greatly distorted making it difficult to define the position of the front as described above.

To present an idea of the movement of the fronts with increasing voltage, we adopt the following method. The position of a point on the edge of one of the birefringent interfaces is monitored as a function of voltage during both ramp up and ramp down until the front containing the reference point merges with the other, advancing front. The scaled position, X, of the point is obtained by dividing the actual position by g. Then, $X = 1$ and $X = 0$ correspond to the reference electrode and the plane at $x = 0$, respectively. Figure 8 is a plot of X *versus* V^2 for two different frequencies. As the fronts undergo considerable distortion and as they do not merge at all points at the same voltage, the curve that is obtained will depend critically on the location of the reference point on the given front. It is thus found (Fig. 8a) that at a higher frequency, the front in the vicinity of the reference point suffers a merger well before the point has neared $x = 0$. At a lower frequency, however, the reference point is closer to $x = 0$ when the fronts coalesce (Fig. 8b). In both cases, the appearance of hysteresis is clearly visible in the high voltage region (before the merging and after the separation of the two interfaces); the curves are more or less linear in the low voltage range but become non-linear when the fronts near coalescence. The voltage width of this hysteresis is slightly higher at the lower frequency. The corrugations of the fronts become more irregular at lower frequencies. Even with the procedure adopted in this work, the variation of the scaled position of a front with voltage becomes irregular. Hence, results for low frequencies have not been included.

Figure 9 is an enlarged picture of the merging fronts and points to the involvement of interfacial effects in the coalescence and separation of the fronts. It is seen that at the time of merging, the common front develops irregularities on a large scale. This is caused not only because the two advancing fronts are not exactly out of phase along y but also because there

may be a slight difference in their lengths along y. When the two fronts merge, the extra length of a disclination wall has to be sacrificed. This is sometimes seen (Fig. 9b) as an isolated, detached loop which disappears over a period of time. An analogous phenomenon that comes to mind is the detachment of a vertically falling liquid drop from the tip of a tube. In this case, the small liquid volume associated with the excess surface energy is thrown out in the form of one or more tiny droplets [18].

Lastly, we consider the effect of a stabilizing **B** field applied normal to the sample planes. This is done on a cell of 400 μm thickness. Increase in sample thickness lowers the thresholds. Hence, the application of **B** will not raise thresholds to very high voltages. With **B** = 0, the voltage is ramped up at $f = 1500$ until the wavy fronts meet. The voltage is held constant at a slightly higher value (19.35). Now **B** is increased from zero. Up to about

Downloaded by [University of Haifa Library] at 10:37 20 August 2012

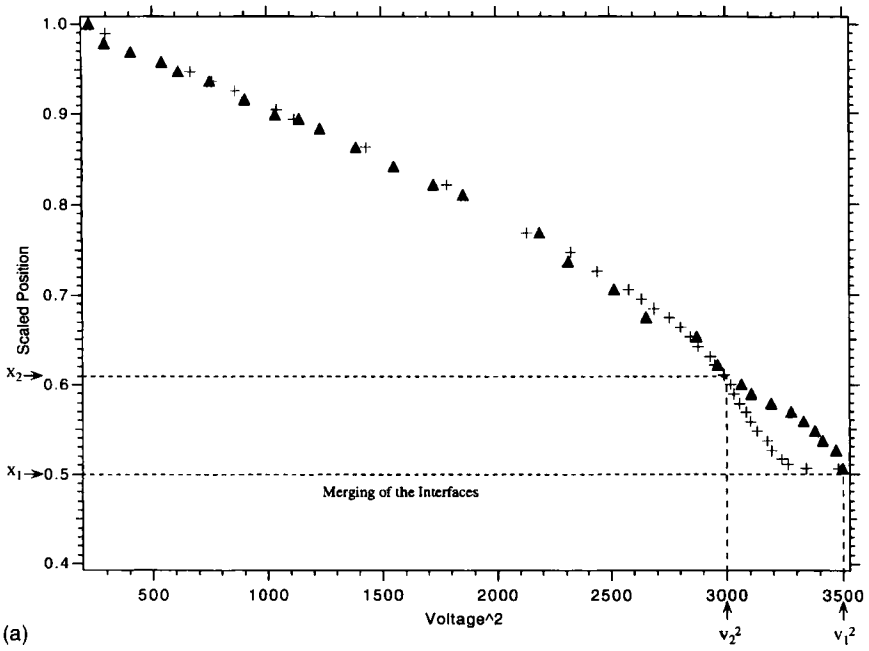

FIGURE 8 Scaled position of the wave front (X) *versus* square of the voltage for (a) $f = 1500$. Ramp up (triangles). Ramp down (+). (b) $f = 500$. Ramp up (circles). Ramp down (crosses). The relevant quantities (X_1, V_1^2, X_2, V_2^2) that demarcate the hysteresis loop are shown. (c) Sample near one electrode (scaled position $X = 1$) showing parameters relevant to the hysteresis width. $X = X_1$ is the scaled position of the common front at $V = V_1$. $X = X_2$ is the scaled position of the front that has receded towards the right electrode at $V = V_2$.

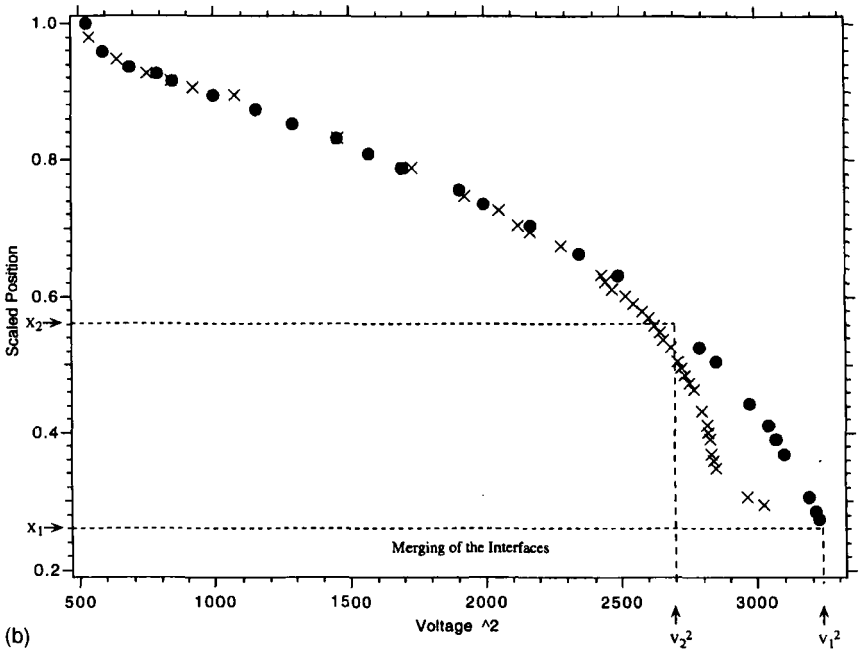

FIGURE 8 (Continued).

$B = 0.44\,\text{kG}$, the **B** field has no perceptible effect. When B exceeds this value, the fronts start to separate out. When **B** is strong enough, say around 1.2 kG, the fronts merge into the respective electrodes leaving the field of view dark – as if no voltage were being applied. From this point, two experiments have been done.

(a) B is diminished in small steps. Till about 0.38 kG, there is no change. Once B is decreased below this point, the birefringent regions start moving towards $x = 0$. Surprisingly, the fronts meet at $B = 0.24\,\text{kG}$, and not at $B = 0$ as anticipated. The waviness of the common front is less uniform than when the increase of B started in the previous cycle. In the course of time, the front dissolves away. Thus, a kind of hysteresis is observed under an increase and a slow diminution of the stabilizing **B**.

(b) **B** is switched off. In this case, the fronts advance towards $x = 0$ at a uniform rate to form the single front. Subsequently, the front dissolves away.

Downloaded by [University of Haifa Library] at 10:37 20 August 2012

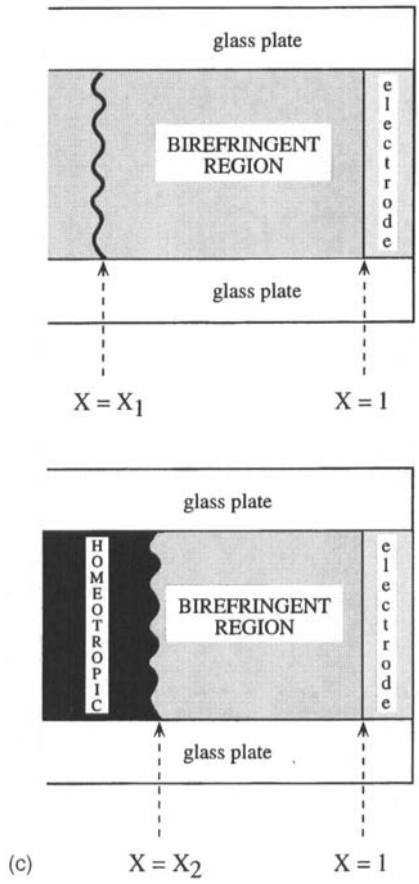

FIGURE 8 (Continued).

3. DISCUSSION

3.1. Hysteresis

Initially, we dwell briefly on the hysteresis of the scaled position of the front (Fig. 8). There are two viewpoints that can be advanced to account for the hysteresis. Firstly, the fronts do not merge at all points at the same voltage. Because of this reason, the fronts cannot be expected to move away from each other at all points when voltage is diminished. The second possibility is that after the fronts have coalesced, they tend to adhere to each other. Hence, they do not separate out as soon as the voltage is diminished by a

Downloaded by [University of Haifa Library] at 10:37 20 August 2012

Downloaded by [University of Haifa Library] at 10:37 20 August 2012

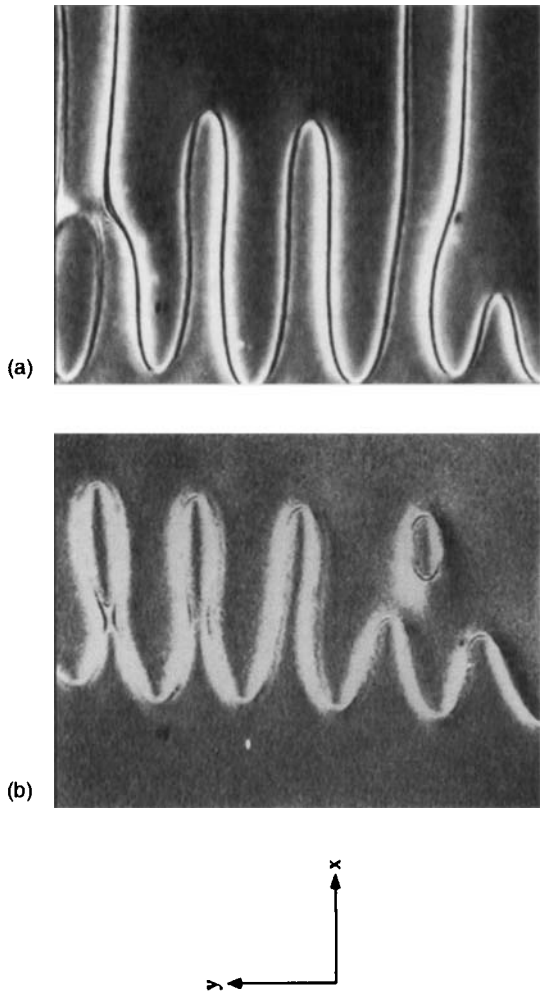

FIGURE 9 (a) and (b) The merging fronts at $f = 1500$ showing irregularities at different parts of the cell. To be noted is the detached disclination loop in diagram (b). $V = 59.17$, $M = 110$. (See Color Plate XVIII).

small amount. Clearly, the adhesion energy is related to the energy represented by the hysteresis loop. If the spatial dependence of the director and electric fields were known, the adhesion energy could be exactly computed by integrating the total free energy density of the sample over the hysteresis loop. In the absence of an exact solution, the energy that is needed to separate the two fronts is estimated below via an order of magnitude

calculation by considering the electrostatic free energy contained in one part of the sample at the extremities of the hysteresis loop.

All nematics exhibit flexoelectricity [19] which gives a contribution of the form

$$W_L = -\mathbf{P} \cdot \mathbf{E}$$

to the free energy density at constant electric potential between electrodes; **P** is the flexoelectric polarization and **E** the electric field. When **E** is time varying, the time average of W_L has to be taken. A characteristic time associated with nematic samples of finite thickness is the viscoelastic relaxation time

$$\tau \sim \frac{\eta d^2}{K}$$

where $\eta (\sim 1$ poise), is an average viscosity coefficient, $d = 2h$, the sample thickness and $K (\sim 10^{-6}$ dyne) an average curvature elastic constant. For a sample of thickness 160 μm, $\tau \sim 100$ sec. It is over a time period of τ that W_L has to be averaged. If f takes values $\sim 10^2$ to 10^3 Hz, W_L becomes negligibly small. Hence, flexoelectricity is ignored.

The dielectric free energy density at constant electric potential is written as

$$W = -\frac{\varepsilon_{jk} E_j E_k}{8\pi}.$$

where ε_{jk} is the anisotropic dielectric tensor; summation over repeated indices is assumed. We try to calculate the electrostatic energy stored in the region of the sample between the front and the nearest electrode. In this region **n** is almost parallel to x. To simplify matters, therefore, we write

$$W \approx -\frac{\varepsilon_{\parallel} E^2}{8\pi}$$

where E is the average electric field strength taken to be $V/(2\,g)$. When the two fronts have just coalesced at $V = V_1$, the free energy density is W_1. We neglect the wavy nature of the fronts and assume that they are parallel to y. Let X_1 be the scaled coordinate of the common front (Fig. 8c). Then, the sample volume between the common front and the reference electrode is

$$v_1 = Tpg(1 - X_1).$$

Downloaded by [University of Haifa Library] at 10:37 20 August 2012

Hence,

$$F_1 = W_1 v_1$$

is the electrostatic free energy stored between the common front and the reference electrode. When the voltage is decreased from V_1, the fronts separate out in such a way that the curve for ramp down joins the curve for ramp up at a lower voltage, V_2 and the front nearest to the reference electrode is at the scaled coordinate X_2 (Fig. 8c) so that the sample volume is now

$$v_2 = Tpg(1 - X_2)$$

The free energy density is W_2 and the free energy stored in the volume v_2 is

$$F_2 = W_2 v_2.$$

The difference in free energy is

$$\Delta F = F_2 - F_1.$$

The area of the front in the yz plane is Tp. We define the adhesion energy per unit area of the front as

$$A = \frac{\Delta F}{Tp}.$$

For $5CB$, $\varepsilon_{\|} = 17.9$ [16]. From Figure 8a, the numerical values are found to be

$$(V_1^2, X_1, V_2^2, X_2) = (3500, 0.5, 3000, 0.62).$$

This leads to $A = 6.3 \times 10^{-3}$ erg cm^{-2} at $f = 1500$ Hz. Similarly, at $f = 500$ Hz (Fig. 8b),

$$(V_1^2, X_1, V_2^2, X_2) = (3250, 0.26, 2700, 0.56);$$

and $A = 1.3 \times 10^{-2}$ erg cm^{-2}. Thus, the adhesion energy density should be $\sim 10^{-3}$ to 10^{-2} erg cm^{-2}. Ignoring the zigzag pattern for the moment, we realize that each advancing front can be regarded as separating regions that contain predominantly homeotropic and homogeneous nematic alignment.

Downloaded by [University of Haifa Library] at 10:37 20 August 2012

Essentially, one side of the front has planar alignment while the other side has homeotropic alignment with respect to z. It is well known [17] that the nematic surface tension has slightly different values, $\gamma_{\parallel}$ and $\gamma_{\perp}$, for planar and perpendicular director alignment, respectively, relative to the surface; the surface anisotropy, $\Delta\gamma \sim 10^{-3}-10^{-2}\,\mathrm{erg\,cm^{-2}}$ which is the same order of magnitude as the adhesion energy density estimated by us.

We now consider the nature of the moving interfaces. Three aspects of the interfaces need to be explained.

(1) Why are the interfaces so sharply demarcated? Why do we not have a uniform change of intensity as we move away from the electrodes towards $x = 0$? Why are there two interfaces that emerge from the two electrodes and move towards $x = 0$? Why is there not just one wall near $x = 0$ that stays stationary all the time?
(2) Why do the interfaces get deformed beyond some voltage?
(3) What is the nature of the zigzag patterns that adorn the interface?

In the absence of a rigorous theoretical description, we attempt to qualitatively answer some of the above questions on the basis of known theoretical and experimental facts. For simplicity, we shall confine our attention to the xz plane. The crux of the matter is the inhomogeneity in **E** which exists even in the absence of a nematic between the two plates. As the plates are charged, the field near the electrodes will be stronger than the field near $x = 0$. This should imply that E_x and E_z are functions of x. As the sample has glass boundaries in two different xy planes, the boundary conditions for **E** and the electric induction, **D**, should ensure that the field is also a function of z. Consider now the nematic between the sample boundaries. Let the applied voltage be low enough. The metal electrodes are untreated and do not impose any specific orientation on the director in the yz plane immediately next to the electrodes. As E_z is strong near the electrodes (*i.e.*, near the yz planes $x = \pm g$), **E** is deviated considerably away from x. This should cause a distortion of the director field away from the homeotropic towards the x axis in the xz plane and result in the two birefringent regions to form next to the two electrodes. As we move away from the electrode towards $x = 0$, E_z becomes weaker, the deviation of **E** away from x becomes less and the director distortion less pronounced. As the director is anchored at the two glass plates, it is clear that the nematic near $x = 0$ must remain unperturbed. This qualitative picture would correspond to a situation where the transmitted intensity which is high near either electrodes, fades away gradually to zero as we move away from either electrode towards $x = 0$.

Downloaded by [University of Haifa Library] at 10:37 20 August 2012

To explain the appearance of the dark wall that forms a sharp partition between the deformed and undeformed regions, we have to invoke previously known results [11] for the bend Freedericksz geometry. It is known [16] that 5*CB* has a high dielectric anisotropy. Suppose a deformation is produced in the *xz* plane by the application of a sufficiently strong **E**. Due to the high dielectric anisotropy of the material, the deformation does not decrease to zero smoothly with a weakening of **E** but does so discontinuously. Experimental proof of the accompanying hysteresis is also available for periodic as well as aperiodic distortions [11]. With this result, we can now envisage the following possibility. Near an electrode the distortion is high. As we move towards $x = 0$, E_z weakens. When E_z falls below a critical limit, the deformation drops sharply to zero. The wall now becomes the sharp cut-off between the deformed and undeformed regions. Clearly, increase of voltage should result in a stronger E_z component and the wall should get pushed towards $x = 0$. Thus, the first question gets answered.

It has ben suggested in [12] that the mechanism for the appearance of undulations in the advancing fronts may be similar to the Carr–Helfrich mechanism [15] that explains the onset of Williams domains in the conduction regime as well as the appearance of the chevron pattern at high electric frequencies in the dielectric regime when a planar oriented nematic sample is subjected to a potential difference between the sample planes. The model of [15] was proposed for a nematic with negative dielectric anisotropy ($\varepsilon_A < 0$) uniformly aligned along x (say) and subjected to a potential difference between two electrodes whose surfaces are parallel to the xy plane. A small director deformation periodic along x will induce charges of opposite sign to segregate at the crests and troughs. When the voltage is low enough, the destabilizing action of E on the charge pockets is annulled by the stabilizing dielectric torque. At a sufficiently elevated voltage, however, a convective instability can set in with a suitable periodicity along x. When f is low, the wavelength of the pattern is of the order of the sample thickness. When f is high enough (dielectric regime), the stripe width is several times smaller than the sample thickness. In a way, this fact matches the observations on the undulation of the fronts as the wavelength of the undulations is about an order of magnitude less than the sample width, p. At this point of time, however, the exact way in which free charge of opposite signs gets segregated at alternate regions along the wall length and how the initially straight wall suffers an undulatory instability above a threshold voltage is not clear to us. This is especially so because the director field changes sharply as we move across the width of a wall. This has also not been clarified in [12].

Downloaded by [University of Haifa Library] at 10:37 20 August 2012

Downloaded by [University of Haifa Library] at 10:37 20 August 2012

Without discounting the above possibility, we qualitatively propose an additional mechanism which may also cause undulations to appear in an initially straight wall. We have already found that the surface tension on either side of the wall can be different by a value $\Delta\gamma$. This means, as we move through a distance w from one side of the wall to the other the surface tension changes by $\Delta\gamma$ leading to a spatial gradient in surface tension, $\gamma' \sim \Delta\gamma/w$ which is of the nature of a volume energy density. Suppose we have a fluctuation in the surface of the membrane. Then the restoring stress on the two sides of the membrane will have different values. When the voltage is increased, w diminishes causing γ' to increase. When γ' increases beyond a critical value, the wall (membrane) which is initially in the yz plane may undergo a transition to a crinkled or crumpled state.

3.2. The Wall

As remarked earlier, the thick dark line in Figures 1–3 appears to be an alignment inversion wall similar to the one studied in [5–7] with **B**. For the sake of completeness, we summarize the theoretical results of [5] for two kinds of walls induced by **B** to enable an interpretation of some the results of this work. Consider first a wall situated normal to **B**. As in [5], cgs units are employed. Let the director be anchored along z between plates $z = \pm h$ with **B** being impressed along x. The plates are assumed to have infinite lengths along x and y. The wall lies in the yz plane situated around $x = 0$ with the splay-bend director deformation confined to the xz plane:

$$\mathbf{n} = (\sin\theta(x,z), 0, \cos\theta(x,z)).$$

Under the assumption of equal splay and bend elastic constants ($K_1 = K_3 = K$), the tilt of n away from the z axis can be shown to be [5]

$$\theta(x,z) = \theta_\infty \tanh\left(\frac{\theta_\infty x}{2\xi}\right)\cos\left(\frac{\pi z}{2h}\right) \tag{1}$$

with ξ, the magnetic coherence length and θ_∞, the amplitude, being given by

$$\xi^{-2} = \frac{\chi_A H^2}{K}$$

$$\theta_\infty^2 = 2\left(1 - \frac{\pi^2\xi^2}{4h^2}\right) \tag{2}$$

where χ_A is the (positive) diamagnetic anisotropy of the nematic and H the magnetic intensity. The wall is assumed to have a thickness w_1 where

$$w_1 \approx \frac{\xi}{\theta_\infty}. \tag{3}$$

Equations (2) and (3) can be recast into the form

$$\frac{1}{w_1^2} = \frac{2\chi_A}{K} H^2 - \frac{\pi^2}{2h^2}; \tag{4}$$

in other words, the inverse square of the wall thickness varies linearly with the square of the magnetic intensity. Clearly the wall thickness is finite and real when $H > H_F$ where

$$H_F = \frac{\pi}{2h}\left(\frac{K}{\chi_A}\right)^{1/2}$$

is the (bend) Freedericksz threshold.

The general variation of distortion (1) can be summarized as follows. At the center of the wall ($x = 0$), θ vanishes; hence, the director is perfectly homeotropic. With respect to variation of x at constant z, θ is antisymmetric. At a given x, θ is symmetric with respect to $z = 0$. It is only within a range $-w_1 \leq x \leq w_1$ that θ strongly depends on x. One can say that between crossed polarizers, the wall will appear as a dark line of approximate thickness w_1. For away from the origin, θ is a function of only z and is given by

$$\theta(\pm\infty, z) = \pm\theta_\infty \cos\left(\frac{\pi z}{2h}\right). \tag{5}$$

The variation of director orientation around the splay-bend wall is shown in Figure 11a for assumed parameters in the plane $z = 0$.

Suppose the wall lies parallel to **B** and is situated around $y = 0$. The director field is assumed to depend upon y and z such that

$$\mathbf{n} = (\sin\theta(y, z), 0, \cos\theta(y, z))$$

In this case, the splay, twist and bend distortions are present. The twist elastic constant enters the picture. Using the same approximations as for the previous case, it is found [5] that the director tilt is described by

$$\theta(y, z) = \theta_\infty \tanh\left(\frac{\theta_\infty y}{2\alpha\xi}\right) \cos\left(\frac{\pi z}{2h}\right); \quad \alpha^2 = \frac{K_2}{K}. \tag{6}$$

Downloaded by [University of Haifa Library] at 10:37 20 August 2012

Downloaded by [University of Haifa Library] at 10:37 20 August 2012

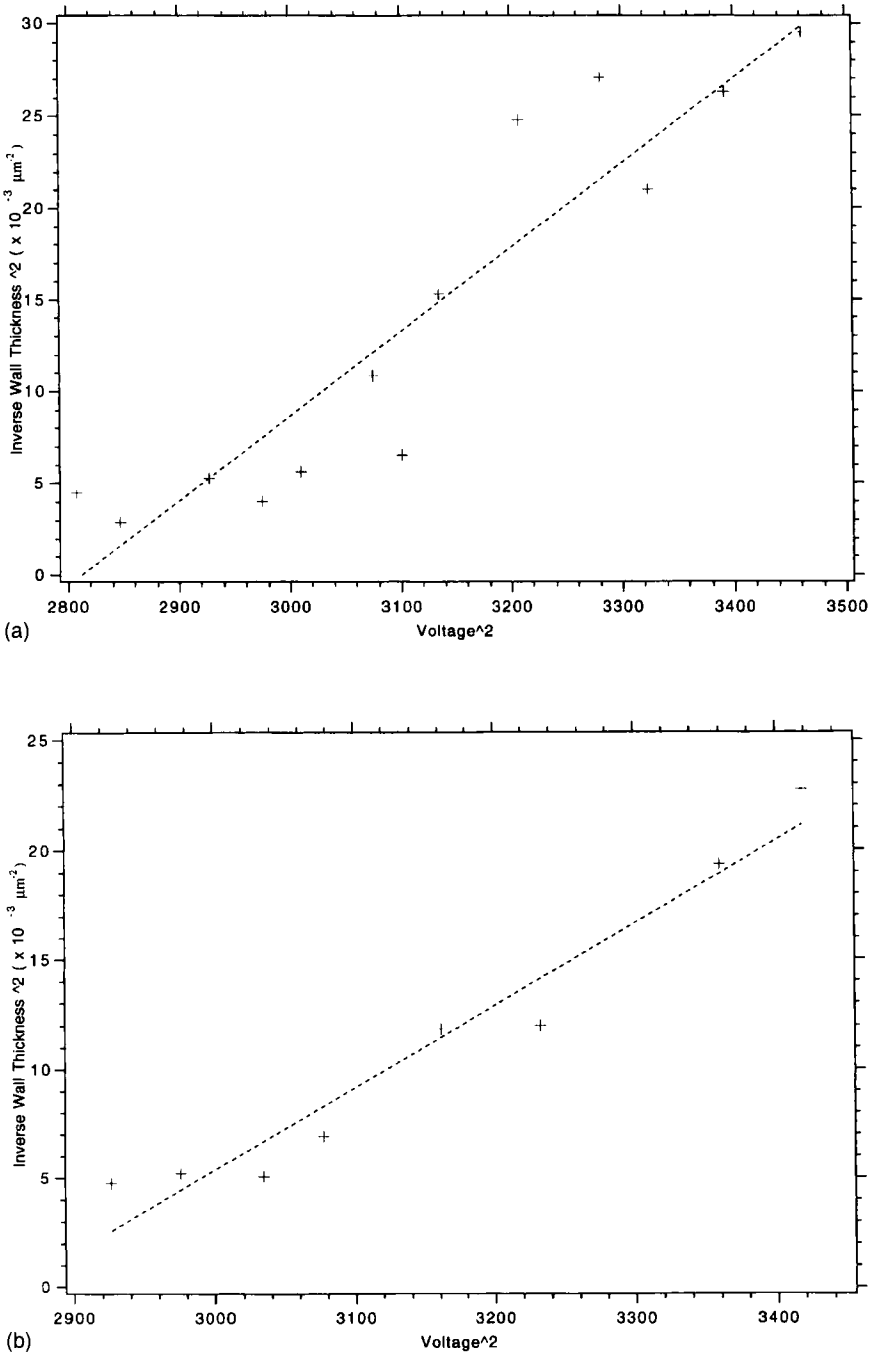

FIGURE 10 Plots of inverse square of wall thickness (w^{-2}) as functions of squared voltage (V^2) for two frequencies. f = (a) 2000 (b) 1500 Hz. The straight line in each case is drawn by a least squares fit.

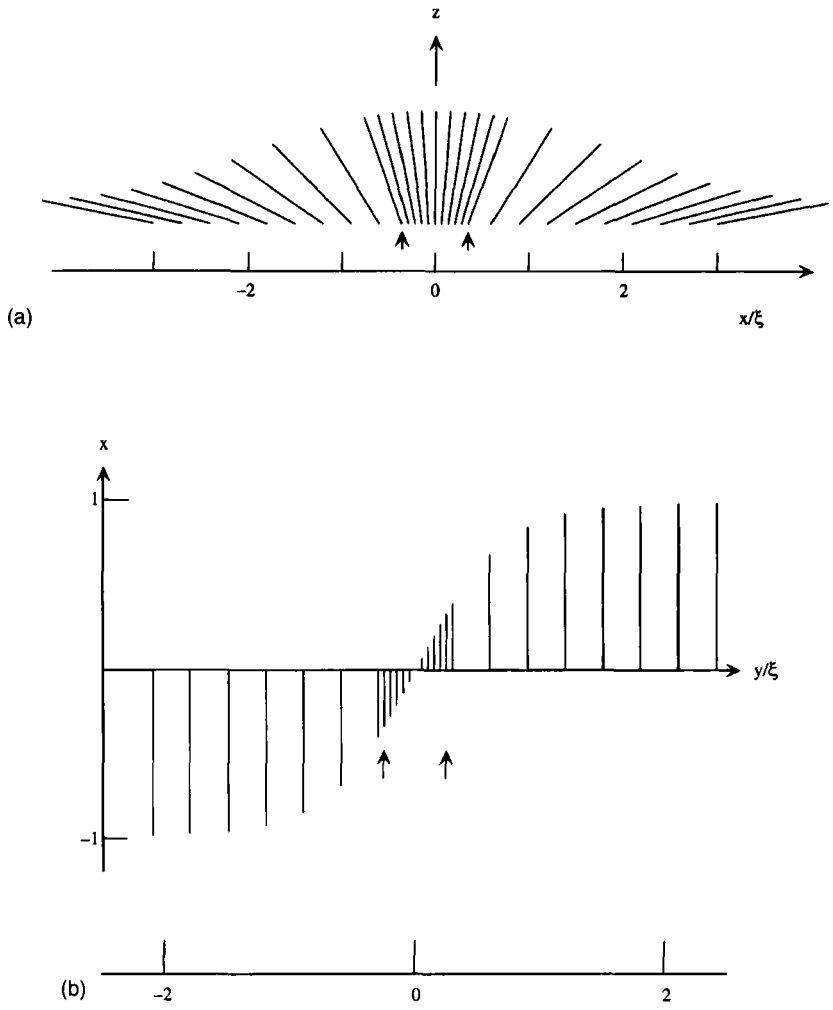

FIGURE 11 (a) and (b). Model calculations of director deformations around walls induced by the **B** field applied along x parallel to the sample. In both cases the plane $z = 0$ is chosen. The walls are situated around the origin. The director is initially homeotropic along z. The sample planes are at $z = \pm h$; $h = 0.01$ cm. $K = 10^{-6}$ dyne is the splay (or bend) elastic constant. The twist elastic constant $K_2 = K/2$; $\chi_A = 10^{-7}$ emu. $H = 10 H_F$ where H_F is the bend threshold. ξ is the magnetic coherence length. The vertical arrows near the origin demarcate each wall whose thickness is defined as in [5]. (a) Splay-bend director deformation in the xz plane due to a wall parallel to the y axis. (b) The wall is parallel to **B**. The director field is projected in the xy plane. The deformation involves bend, splay and twist. (c) Schematic representation of the director distortion in a portion of the curved wall as seen along z axis between crossed polarizers. Other regions such as the zigzag patterns are not shown. The region marked D near each crest appears dark as the director orientation is homeotropic in the center of the wall. Between successive regions D are the regions $L+$ and $L-$ where the wall appears light; here, the director distortion has a twist superposed on the splay and bend. In regions $L+$ and $L-$, the twist of the director away from the homeotropic is in opposite sense.

Downloaded by [University of Haifa Library] at 10:37 20 August 2012

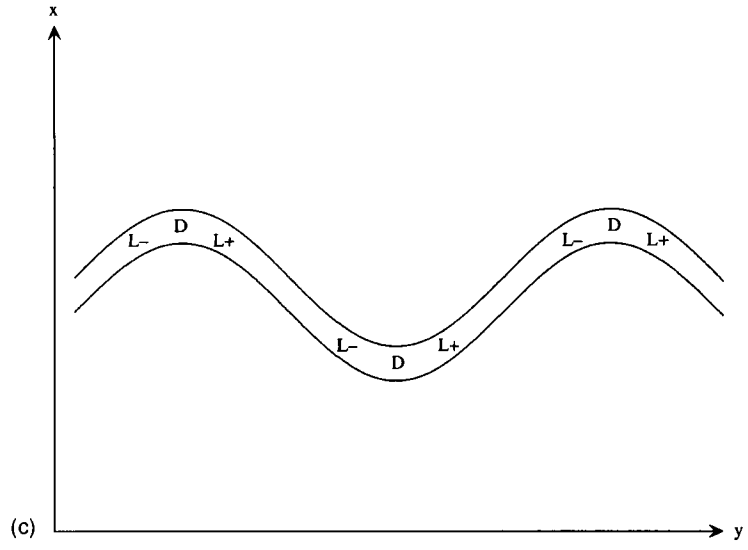

FIGURE 11 (Continued).

Comparing (6) and (1), the wall thickness in the present case becomes

$$w_2 \approx \frac{\xi\alpha}{\theta_\infty}. \tag{7}$$

As K_2 is generally the weakest elastic constant for calamitic nematics, $w_2 < w_1$ for a given magnetic strength. The variation of w_2 with H is similar to that of w_1:

$$\frac{1}{w_2^2} = \frac{1}{\alpha^2}\left[\frac{2\chi_A}{K}H^2 - \frac{\pi^2}{2h^2}\right]. \tag{8}$$

The qualitative nature of the variation of θ Eq. (6) in this case is similar to that of Eq. (1). At the center of the wall, the director is homeotropic. At a given y, θ is symmetric with respect to $z = 0$. At sufficiently large distances from the wall, θ is given by (5) and is a function of z alone. At constant z, θ is antisymmetric with respect to y variation. The projection of the director in the xy plane changes sign as we cross the origin showing a clear signature of the superposed twist deformation as depicted in Figure 11b.

In the present case, the electric field is the destabilizing agent. Rough estimates made from Figures 2 and 5b show a diminution in wall thickness

Downloaded by [University of Haifa Library] at 10:37 20 August 2012

with increase in voltage. This creates the motivation to find out whether the inverse square of the wall thickness varies linearly with the square of the applied voltage. This task is not straightforward because of the following reasons. The wall described in [5] is straight while in the present work the wall is curved in the xy plane. The thicknesses of a magnetic field induced wall (Eq. 3 or 7) is the same along the length of the wall but the walls found in Figures 1–3, 5, 7 have different thickness at different points. This means the wall thickness will have to be measured at a number of points along the wall and the average taken. In addition, a single wall tends to split into two parts away from a crest (Fig. 5b) at certain voltages. But the wall generally remains unsplit near the crests. To simplify the procedure, we choose a point near one of the crests and follow the crest as the voltage is increased. At a given voltage, the video image of the crest is enlarged and printed out. Then the wall thickness near the crest (w) is measured using a traveling microscope. It is difficult to measure the wall thickness close to the coalescence voltage. The plots of w^{-2} as functions of V^2 are shown for two frequencies in Figure 10 and in each case the best fitting straight line is drawn. It is found that the points are distributed about the straight line. We do not present results for lower frequencies as the variation becomes more erratic.

The nature of director distortion along a curved wall can be properly understood only by making detailed conoscopic observations. At this stage it is difficult to give detailed diagrams of the director field inside the wall at different points. Tentatively, however, we can deduce the variation of director tilt using the results of (l)–(8) and Figures 11a and 11b. Figure 11c represents a portion of the curved wall seen along z. The parts D and L are dark and light, respectively, between crossed polarizers (see Fig. 5b). The regions D are close to the crests whose tangents are parallel to the electrodes (*i.e.*, parallel to the y axis). By ignoring the distortion in the electric field, we can say that the wall at D is *normal* to the electric field (Fig. 11a). At D, the wall is of the splay-bend type and the distortion is a function of x and z; a twist deformation is absent inside the wall. Between two neighbouring crests D, the wall is inclined to the field. By tilting away from the y axis, the wall tends to acquire properties of one that lies parallel to the field (Fig. 11b). In other words, the director field inside the wall suffers a twist in addition to splay and bend as we move away from D. But we know that at D there can be no twist. The picture that emerges now is the following. Let us start with the first region D and move along the wall in the general direction of $+y$. At a point removed from D, the director inside the wall twists away from z in one sense. We call this region $L+$. On further traversing along the wall, the twist angle increases and becomes a maximum. When we move further, the

Downloaded by [University of Haifa Library] at 10:37 20 August 2012

twist angle diminishes (region $L-$) and finally goes to zero when we reach the next crest (D). This ensures that the average amount of twist in a given part of the wall between two neighbouring crests is zero – as it should because the nematic is non-chiral. When we move from the second crest to the third, the process repeats. We see that the sense of twist is opposite on either side of a given crest D. Thus, the average twist in the neighbourhood of any crest also remains zero. We remember that the wall thickness w_2 Eq. (7) is smaller than the thickness w_1 when twist is absent. As the twist appears and disappears at different points along the length of the wall, the wall thickness measured at different points of the wall may also be different.

Downloaded by [University of Haifa Library] at 10:37 20 August 2012

4. CONCLUDING REMARKS

In conclusion, the main features of the observations of [12] have been reproduced in thicker samples. Some new results have been reported. Each interface that separates out of an electrode with increasing voltage not only contains a dark wall but is also lined by zigzag defect patterns. The zigzag patterns are different from the zigzag disclinations reported in [8–10]. Hysteresis is observed when the voltage is diminished after the fronts have merged near $x=0$. This is interpreted as caused by the adhesion of the two interfaces. Neglecting flexoelectricity, an order of magnitude estimate is made from which the surface density of adhesion energy is found to be of the same order as the surface tension anisotropy normally measured for nematics. When the electric frequency is low enough, the wall thickness and the positions of the fronts vary less regularly with voltage; this indicates the possible role of electrical conductivity at low f. After the fronts coalesce, the application of a sufficiently strong stabilizing **B** along z causes the interfaces to separate and retreat towards the two electrodes leaving the entire field of view dark corresponding to homeotropic alignment. It is thus established that the merging of the two fronts is accomplished above an electric threshold and that the threshold is raised in the presence of a stabilizing **B**. Detailed work on this has not been reported, such as effects of the variation of magnetic tilt. The cause of the appearance of the zigzag defect patterns is not known to us. The curving of the initially straight advancing interfaces is qualitatively accounted for as being due to an instability caused by two factors – the difference in surface energy density on the two sides of the wall and the decreasing wall thickness with increasing voltage.

Each front includes a wall across which the director orientation appears to change sharply. Due to reasons stated in the text, accurate measurement of the wall thickness cannot be made. The available data shows that the wall

thickness diminishes as the fronts approach each other (*i.e.*, with increasing voltage). This is in qualitative agreement with earlier observations [5, 6] on magnetic field induced walls. The results of [5] are useful in providing an approximate picture of the director orientation around the wall (Fig. 11), but the reason for the splitting of the wall away from the crests (Fig. 5b) is not yet known. A plot of the square of the inverse wall thickness does not vary sufficiently linearly with the square of the voltage. To this extent, the behavior of walls in the present case is different from that of the **B** induced walls [5, 6]. A possible explanation for this is the following.

The mathematical model of [5] contains only one governing equation for the director tilt angle. A similar analysis [20] shows that even in a situation where the director deforms only in the xz plane and a single angle, θ, describes the distortion, it is necessary to include the modification of the electric field by considering ψ, the local perturbation of the electric potential. Even the simplifying assumptions of [5] result in a set of coupled differential equations in θ and ψ which do not have an analytical solution of the kind deduced in [5]. As 5*CB* has very high dielectric anisotropy, the coupling between ψ and θ is strong. Hence, the variation of w with voltage may not follow a rule that is qualitatively similar to (4) or (8). The results of a numerical solution of the complete set of governing equations will be communicated in the future.

Some directions for future studies become apparent by a comparison of the present results with those of [12]. For instance, no hysteresis is reported in [12]. As the samples used in [12] are thinner than those employed here, one may tentatively conclude that there may exist some critical sample thickness such that for thicknesses higher than this value, hysteresis is observable. At the same time, the differences in the preparation of cells must be borne in mind. In [12], thin electrodes or wire electrodes are employed while in the present study the electrodes are flat plates. In both cases the metal surfaces are not coated with surfactant to induce better director anchoring at the electrodes, but the materials of the electrodes may be different. As results obtained with uncoated metal electrodes may not always be reproducible (especially at low frequencies) due to various electrochemical processes, it may be advisable to coat the surfaces of flat electrodes for homogeneous anchoring along z. This will be done in future experiments so that results for coated metal electrodes can be compared with those obtained in this work.

It has not been possible to systematically study the role of electrical conductivity. The erratic behavior of different measured quantities at low frequencies is a clear indication that conductivity effects may become

Downloaded by [University of Haifa Library] at 10:37 20 August 2012

important when f is lowered below some limit. Each nematic has a distinct conductivity anisotropy, the magnitude and sign of which can be altered by the addition of suitable impurities. It should be interesting to study the effect of the addition of conducting impurities on the different measurable quantities (wall thickness, undulation frequency of the fronts, the scaled position of fronts, *etc.*) in our experiments.

A different line of study is indicated by the theoretical interpretation of Section 3. Assuming that this is acceptable, then the appearance of sharp walls is due to the nematic with high, positive ε_A being subjected to an inhomogeneous **E** [11]. Suppose the material studied has low, positive ε_A. (The question now is, whether the sharp walls will again appear or whether the deformation that sets in near the electrodes at some voltage will gradually go to zero as we move towards $x = 0$. This possibility can be tested either by repeating the experiments with *5CB* at a higher temperature or by using a nematic with low, positive ε_A. The suspected existence of twist in parts of the curved wall (Figs. 5b and 11) suggests a different experiment. It is known that some nematics that change into smectic A at lower temperatures exhibit anmalously high values of K_3 and K_2. Experiments on such materials will indicate in what way divergence of these curvature elastic constants will affect the formation and curving of walls.

Lastly, we remember that *5CB* is a material with positive diamagnetic anisotropy so that the magnetic field applied along z tends to increase the destabilizing electric threshold. There do exist nematics with negative χ_A but positive ε_A. If such a nematic is studied, a magnetic field applied along z will tend to destabilize the initial homeotropic orientation. Experiments on nematics having opposite signs of dielectric and diamagnetic anisotropies should prove interesting.

Downloaded by [University of Haifa Library] at 10:37 20 August 2012

Acknowledgments

Bramley acknowledges support provided by the National Science Foundation through an REU grant DMR 9322301. Garg would like to thank Dr. Oleg Lavrentovich of the Liquid Crystal Institute for helpful discussions at the early stages of this work. The authors thank a referee for useful comments on an earlier version of this work.

References

[1] D. Demus and L. Richter, Textures of Liquid Crystals (VEB, Leipzig, 1978).
[2] M. Kleman, Points, Lines and Walls: in Liquid Crystals, Magnetic Systems and Various Ordered Media (John Wiley, Chichester, 1983).

[3] R. Williams, *Phys. Rev. Lett.*, **21**, 342 (1968).
[4] W. Helfrich, *Phys. Rev. Lett.*, **21**, 1518 (1968).
[5] F. Brochard, *J. de Physique*, **33**, 607 (1972).
[6] L. Leger, *Solid State Cammun.*, **10**, 697 (1972); *ibid*, **11**, 1499 (1972); *Molec. Cryst. Liquid Cryst.*, **24**, 33 (1973).
[7] A. Stieb, G. Baur and G. Meier, *J. de Physique Colloq. C1*, Suppl. 3, **36**, C1–185 (1975).
[8] Y. Galerne, J. Itoua and L. Liebert, *J. Phys. France*, **49**, 681 (1988).
[9] Y. Galerne and L. Liebert, *Phys. Rev. Lett.*, **55**, 2449 (1985).
[10] M. Mihailovic and P. Oswald, *J. Phys. France*, **49**, 1467 (1988).
[11] B. J. Frisken and P. Palffy-Muhoray, *Phys. Rev.*, **A39**, 1513 (1989); *ibid*, **A40**, 6099 (1989); *Liquid Crystals*, **5**, 623 (1989); U. D. Kini, *Liquid Crystals*, **8**, 745 (1990).
[12] K. T. Schell and R. S. Porter, *Molec. Cryst. Liquid Cryst.*, **174**, 141 (1989).
[13] S. Garg, S. Saeed and U. D. Kini, *Phys. Rev.*, **E51**, 5846 (1995).
[14] S. Garg, S. Wild, B. Zurn, S. Saeed and U. D. Kini, *Liquid Crystals*, **24**, 501 (1998).
[15] E. F. Carr, *Molec. Cryst. Liquid Cryst.*, **7**, 253 (1969); W. Helfrich, *J. Chem. Phys.*, **51**, 4092 (1969); E. Dubois-Violette, P. G. de Gennes and O. Parodi, *J. de Physique*, **32**, 305 (1971).
[16] P. G. Cummins, D. A. Dunmur and D. A. Laidler, *Molec. Cryst. Liquid Cryst.*, **30**, 109 (1975). At 28°C, $\varepsilon_{\parallel} = 17.86$ and $\varepsilon_{\perp} = 7.25$ are the dielectric constants along and normal to the director, respectively.
[17] J. Cognard, *Molec. Cryst. Liquid Cryst. Suppl.*, **1**, 1 (1982).
[18] J. W. Williams and R. A. Alberty, In '*A Treatise on Physical Chemistry*', Volume 2, Edited by H. S. Taylor and S. Glasstone (D. Van Nostrand, Princeton, 1952), pp. 571–2.
[19] R. B. Meyer, *Phys. Rev. Lett.*, **22**, 918 (1969); J. Prost and J. P. Marcerou, *J. Phys. France*, **38**, 315 (1977); G. Durand, *Mol. Cryst. Liquid Cryst.*, **113**, 237 (1984).
[20] Unpublished results.

Downloaded by [University of Haifa Library] at 10:37 20 August 2012